Structure and Kinetics of Aggregating κ-Carrageenan Studied by Light Scattering

Vincent Meunier, Taco Nicolai,* and Dominique Durand

Chimie et Physique des Matériaux Polymères, UMR-CNRS 6515, Université du Maine, 72085 le Mans Cedex 9, France

Received August 23, 1999; Revised Manuscript Received January 31, 2000

ABSTRACT: We have studied the evolution in time of the structure factor of aggregating κ-carrageenan using light scattering. Aggregation was induced by cooling solutions containing 0.01 M KCl below a critical temperature. The ionic strength of the solutions was fixed by adding 0.1 M NaCl. Large aggregates consist of locally rigid bundles formed by parallel aggregation of κ-carrageenan. The effect of concentration ($C <$ 0.3 g/L) and temperature on the structure was found to be small. The aggregation rate increases with increasing concentration and decreasing temperature. The optical rotation, i.e., the helix content, is not influenced by aggregation. The molar mass, size, and interactions of nonaggregated κ-carrageenan were determined in the coil and the helix state. For the large molar sample used in this study ($M_w = 4.2 \times 10^5$ g/mol) the molar mass and the size are almost the same in the coil and the helix state.

Introduction

The carrageenans are a family of linear sulfated galactans extracted from various species of marine red algae. Different types may be distinguished by their primary structures.[1] κ-Carrageenan is composed of alternating α(1−3)-D-galactose-4-sulfated and β(1−4)-3,6-anhydro-D-galactose. This polysaccharide is used in the food industry as a gelling agent.[2,3] It forms a thermoreversible gel on cooling below the temperature (T_c) where the conformation changes from a random coil to a helix.[4,5] The temperature, the ionic strength, and the nature of the counterions regulate this conformational change and, consequently, the gelation process.[6,7]

The precise mechanism of the salt-induced gelation of κ-carrageenan continues to be a matter of debate and controversy. Although there is agreement on a two-step mechanism of gelation, i.e., a coil−helix transition followed by aggregation of the helices, the exact nature of these helices and the way the gel is formed are not yet established.[5,8−11]

The local structure of the aggregates and the gel has been studied by X-ray scattering in an attempt to elucidate the helical structure.[12−14] The large-scale structure has been studied using microscopy.[15,16] It was observed that in the presence of specific counterions κ-carrageenan forms rigid-rod-like aggregates on cooling below T_c. On the other hand, in the presence of iodide, a specific co-ion, helices are formed, but aggregation is inhibited. However, recently, Bongaerts et al.[17] have suggested that κ-carrageenan reversibly associates at iodide concentrations of 0.2 M and higher.

In previous work, we have studied the evolution in time of the shear modulus and the scattered light intensity of aqueous κ-carrageenan solutions at various concentrations and temperatures;[18] the aim of the present work is to study the evolution of the structure of aggregating κ-carrageenan and to investigate the influence of temperature and concentration. Light scattering is very sensitive to the presence of aggregates and is therefore a powerful method for studying the initial stages of aggregation even at very low concentrations.

Light scattering has been used in the past to characterize κ-carrageenan[19,20] but not to study its aggregation. Ueda et al. studied the molar mass distribution of κ-carrageenan in KCl, i.e., in conditions where it aggregates. However, they investigated the solutions immediately after lowering the temperature below T_c assuming implicitly that the aggregation is completed in a short time. From our previous study it is clear that in fact they analyzed only the rather small aggregates formed in the early stages of the aggregation process. The reversible association in iodide reported by Bongaerts et al.[17] is different from the irreversible aggregation that occurs in the presence of specific counterions. Of course, the aggregation can still be reversed by raising the temperature, but at a fixed temperature below T_c the aggregation is a continuous process and an equilibrium is not observed.

We also will give a full characterization of the κ-carrageenan used for this study in the coil conformation and the nonaggregating helix conformation. A hotly disputed issue is whether κ-carrageenan forms single or a double helices, and still very recently both the single[21] and the double helix[22] have been forcefully defended in the literature. In the characterization presented here we do not find support for the double helix, but the objective of this paper is not to further investigate this issue. Here we want to study the aggregation process that leads to gel formation. We do not think that it is very important whether the large aggregates are built up from double or single helices.

Experimental Section

Methods. Light scattering measurements were made using an ALV-5000 multibit, multi-τ full digital correlator in combination with a Malvern goniometer and a Spectra-Physics laser emitting vertically polarized light at $\lambda = 532$ nm. The temperature is controlled by a thermostat bath to within ±0.1 °C. Measurements were done over short periods of time at several angles of observation (θ). This series of measurements was repeated during the aggregation process for at least 10 h. The relative excess scattering intensity (I_r) was calculated as the total scattered light intensity minus the solvent scattering divided by the scattering intensity of toluene at 20 °C.

10.1021/ma991433t CCC: $19.00
Published on Web 03/17/2000

In general, I_r can be written as[23]

$$I_r = KCM_w S(q) \tag{1}$$

where $S(q)$ is the structure factor which expresses the scattering wave vector dependence of the scattering intensity ($q = 4\pi n_s \sin(\theta/2)/\lambda$, with θ the angle of observation and n_s the refractive index of the solution) and K is a contrast factor:

$$K = \frac{4\pi^2 {n_s}^2}{\lambda^4 N_a}\left(\frac{\partial n}{\partial C}\right)^2\left(\frac{n_{tol}}{n_s}\right)^2\frac{1}{R_{tol}} \tag{2}$$

Here N_a is Avogadro's number, $(\partial n/\partial C)$ is the refractive index increment, and R_{tol} is the Rayleigh ratio of toluene at 20 °C (2.79×10^{-5} cm^{-1} at $\lambda = 532$ nm[24]). $(n_{tol}/n_s)^2$ corrects for the difference in scattering volume of the solution and the toluene standard with refractive index n_{tol}. In the calculation of K we have used $\partial n/\partial C = 0.145$ close to the value reported in ref 19. Direct measurement gave $\partial n/\partial C = 0.128$, but heating under vacuum at 90 °C for 6 h showed that the water content in the κ-carrageenan powder is between 15 and 20%. Since we determine the concentration also by refractometry, the error in the absolute value of M_w is directly proportional to that in $\partial n/\partial C$. The choice of the exact value of $\partial n/\partial C$ is not so important, as long as one corrects for the differences when comparing with literature results. We measured the intensity of a κ-carrageenan solution in 0.1 M NaCl, i.e., in the coil state over a range of temperatures between 15 and 40 °C. The variation of the scattered light intensity and thus the refractive index increment is negligible in this temperature range.

$S(q)$ depends on the structure of the solute and on the interactions. Using the so-called Zimm approximation, eq 1 can be written in terms of the static correlation length (ξ) and the z-average second virial coefficient (A_2) if higher-order terms in C and in $q\xi$ can be neglected:[23]

$$\frac{KC}{I_r} = \frac{1}{M_w}(1 + 2A_2M_wC)(1 + (q\xi)^2) \tag{3}$$

With dynamic light scattering (DLS) the intensity autocorrelation function is measured which is related to the field autocorrelation function via the so-called Siegert relation.[25] For dilute solutions of monodisperse particles with $qR_g < 1$, the normalized field correlation function ($g_1(t)$) is a single-exponential decay with relaxation time $\tau = (q^2D)^{-1}$, where D is the translational diffusion coefficient. D is related to the hydrodynamic radius R_h via the so-called Stokes−Einstein relation:

$$D = \frac{k_BT}{6\pi\eta R_h} \tag{4}$$

with k_B Boltzmann's constant, T the absolute temperature, and η the solvent viscosity. For polydisperse dilute solutions $g_1(t)$ is characterized by a distribution of relaxation times ($A(\tau)$):

$$g_1(t) = \int A(\log \tau)\exp(-t/\tau)\, d\log \tau \tag{5}$$

The relaxation time distribution is obtained as a function of log τ because the correlation function itself is measured on a logarithmic time scale. Computer routines such as REPES and CONTIN[26] can be used to obtain the relaxation time distribution without assuming a specific shape. With this method we obtain relatively narrow single peaked distributions. We never observed a second peak at longer relaxation times, which would imply the presence of aggregates. However, the problem with these routines is that a smoothing procedure on the distribution is used to avoid unrealistic detail in the shape of $A(\log \tau)$. This smoothing does not influence the averages but tends to favor more symmetric distributions. Therefore, we force fitted the data to the so-called generalized exponential distribution:[27]

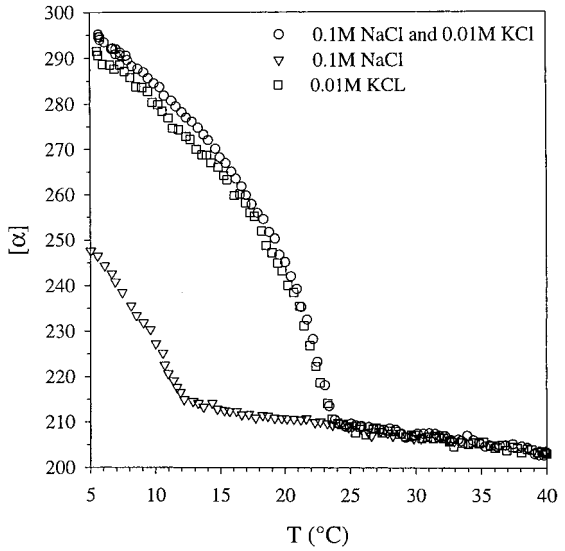

Figure 1. Temperature dependence of the specific optical rotation of κ-carrageenan solutions in 0.1 M NaCl, 0.01 M KCl and in 0.1 M NaCl plus 0.01 M KCl.

$$A(\log \tau) = k\tau^p \exp[-(\tau/\tau^*)^s] \tag{6}$$

This versatile function contains two parameters (p, s) to describe the shape of a wide range of single peaked distributions such as the Schultz−Zimm and the Pearson distribution. τ^* is the characteristic relaxation time, and k is a normalization constant.

Optical rotation measurements were made using a Perkin-Elmer 341 polarimeter. All measurement were made at $\lambda =$ 365 nm (Hg lamp) using a thermostated cell (optical path length 10 cm).

The apparatus used for size exclusion chromatography (SEC) with on-line light scattering detection is described in ref 28. We used the following two columns in series: TSK PW 5000 (30 cm) and TSK PW6000 (60 cm). The eluent was 0.1 M $NaNO_3$. We injected 300 μL of solution with sufficiently low concentration ($C = 0.2$ g/L) so that interactions are negligible.

Materials. The κ-carrageenan used for this study is an alkali-treated extract from *Eucheuma cottonii* supplied by SKW Biosystems, (Baupte, France). Note that the sample is not the same as the one used in our previous study.[18] NMR measurements in NaCl were done at 90 °C in order to estimate the amount of ι-carrageenan. We found that the sample contains at most a few percent ι-carrageenan. SEC with on-line light scattering detection gave weight-average molar mass $M_w = 3.8 \times 10^5$g/mol and polydispersity index $M_w/M_n = 2$.

The solutions were prepared as follows. A freeze-dried sample of κ-carrageenan in the sodium form was dissolved while stirring a few hours in hot Millipore water (70 °C) with 200 ppm sodium azide added as a bacteriostatic agent. The pH was adjusted to 9 to eliminate the risk of hydrolysis during preparation.[29−31] The solution was dialyzed against Millipore water to eliminate excess salt. Hot Millipore water containing 0.2 M NaCl and 0.02 M KCl was added to set the final ionic conditions at 0.1 M NaCl and 0.01 M KCl. We chose a concentration of 0.01 M KCl in order to have a convenient coil−helix transition temperature close to ambient.[32] NaCl was added to screen electrostatic interactions and to make the ionic strength independent of the κ-carrageenan concentration. We found that the temperature (T_c) below which the optical rotation increases abruptly is 24 °C with and without the presence of 0.1 M NaCl in addition to 0.01 M KCl; see Figure 1. Usually the transition midpoint temperature is used to characterize the coil−helix. However, the initial abrupt rise is a better measure of the critical temperature where aggregation starts. The solutions always contained a small amount of large aggregates which perturb the light scattering results.

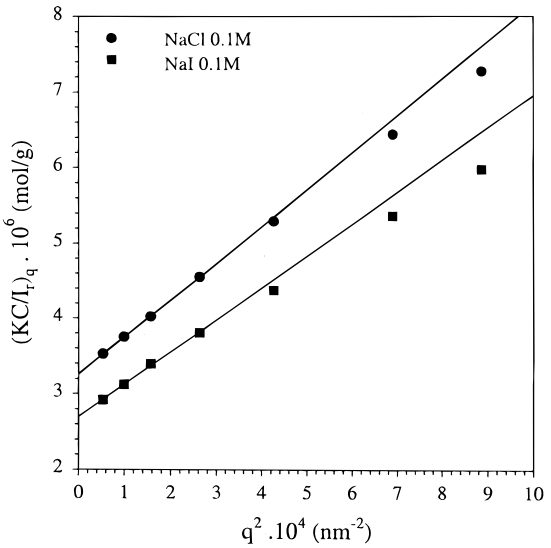

Figure 2. Dependence of KC/I_r on q^2 of κ-carrageenan solutions at $C = 0.1$ g/L in 0.1 M NaCl and 0.1 M NaI at 20 °C. The solid lines represent linear least-squares fits to the four smallest values.

These aggregates were removed by filtration through 0.2 μm pore size Anotop filters. The absence of aggregated material and other spurious scatterers was checked by dynamic light scattering. The solutions were stored at 50 °C.

For the characterization of nonaggregated κ-carrageenan solutions were prepared in the same way with ionic strengths 0.1 M NaCl or 0.1 M NaI.

Results and Discussion

Characterization of κ-Carrageenan in the Coil and Helix Conformation. The κ-carrageenan used in this study was characterized at 20 °C using static and dynamic light scattering. Optical rotation shows that at 20 °C κ-carrageenan has a coil conformation in the presence of 0.1 M NaCl and almost the maximum helix conformation in the presence of 0.1 M NaI.

Figure 2 shows KC/I_r as a function of q^2 at $C = 0.1$ g/L. The curvature at higher values of q^2 demonstrates the limitation of eq 3. Note that the curvature is less marked at higher concentrations because ξ is smaller. Linear least-squares fits of the data at low q values give ξ.

Figure 3a shows the concentration dependence of KC/I_r extrapolated to $q = 0$ from which we obtain $M_w = 4.2 \times 10^5$ g mol^{-1} and $A_2 = 4.5 \times 10^{-3}$ mL mol g^{-2} in NaCl and $M_w = 4.3 \times 10^5$ g mol^{-1} and $A_2 = 1.9 \times 10^{-3}$ mL mol g^{-2} in NaI. The concentration dependence of ξ is shown in Figure 3b and is more important in NaCl than in NaI. At infinite dilution ξ is proportional to the z-average radius of gyration ($R_{gz} = \sqrt{3}\xi$). Extrapolation to $C = 0$ gives $R_{gz} = 72$ nm in NaCl and $R_{gz} = 74$ nm in NaI.

The cooperative diffusion coefficient was determined using the average relaxation rate ($\Gamma = 1/\tau$) obtained from DLS measurements: $D_c = \langle\Gamma\rangle/q^2$. As $\langle\Gamma\rangle/q^2$ has a weak q dependence due to polydispersity, rotation, and internal motion, we used the value extrapolated to $q = 0$. D_c has a linear concentration dependence over the range investigated; see Figure 4:

$$D_c = 7.0 \times 10^{-8}(1 + 0.776C) \quad \text{in 0.1 M NaCl} \qquad (7a)$$

$$D_c = 7.0 \times 10^{-8}(1 + 0.304C) \quad \text{in 0.1 M NaI} \qquad (7b)$$

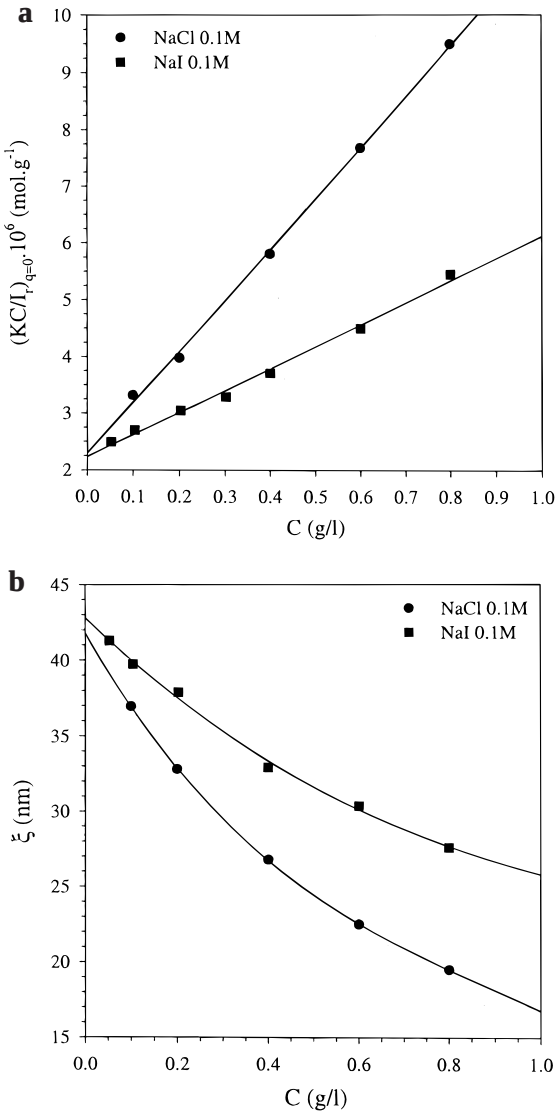

Figure 3. (a) Concentration dependence of KC/I_r extrapolated to $q = 0$ of κ-carrageenan solutions in 0.1 M NaCl and 0.1 M NaI at 20 °C. The solid lines represent linear least-squares fits. (b) Concentration dependence of the static correlation length of κ-carrageenan solutions in 0.1 M NaCl and 0.1 M NaI at 20 °C. The solid lines are guides to the eye.

The z-average hydrodynamic radius, R_{hz}, can be calculated from D_c extrapolated to $C = 0$ via eq 4: $R_{hz} = 30$ nm both in NaCl and in NaI. Note that R_{hz} represents $1/\langle R_h^{-1}\rangle_z$, while R_{gz} obtained from SLS represents $\sqrt{\langle R_g^2\rangle_z}$, and therefore the latter more strongly weighs large particles.

If we assume that the relaxation time distribution simply reflects the distribution of the hydrodynamic radii, we can determine the latter by calculating R_h corresponding to each relaxation time using eq 4. This assumption is justified at sufficiently low concentration and scattering angle so that the effects of interactions and internal dynamics can be neglected.

In Figure 5 we compare the size distribution of κ-carrageenan in the coil and helix conformation. Note that the area under the curve is proportional to the scattered light intensity, which means that large particles are strongly weighed. At the concentration ($C = 0.1$ g/L) and scattering wave vector ($q = 0.01$ nm^{-1}) used, the effects of interactions and internal dynamics are small. Clearly, there is remarkably little difference

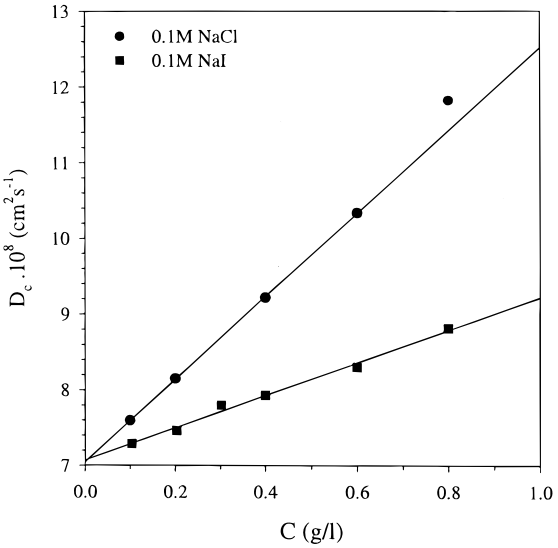

Figure 4. Concentration dependence of the cooperative diffusion coefficient of κ-carrageenan solutions in 0.1 M NaCl and 0.1 M NaI at 20 °C. The solid lines represent linear least-squares fits.

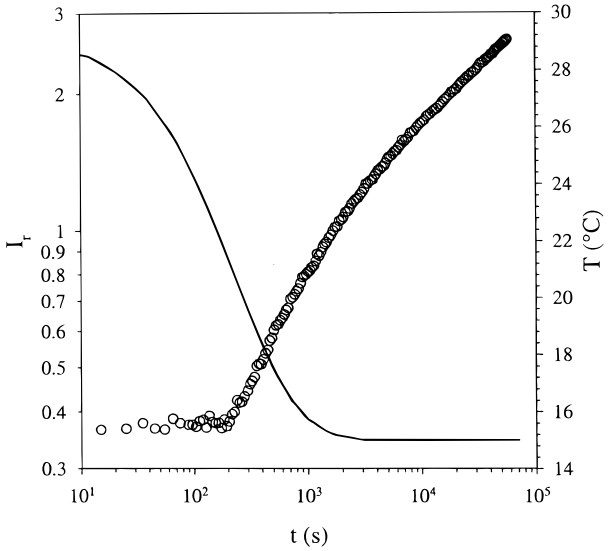

Figure 6. Evolution of the relative excess scattering intensity (C = 0.1 g/L, $q = 1.26 \times 10^{-2}$ nm^{-1}, T = 15 °C, 0.01 M KCl, 0.1 M NaCl). The solid line indicates the time dependence of the temperature.

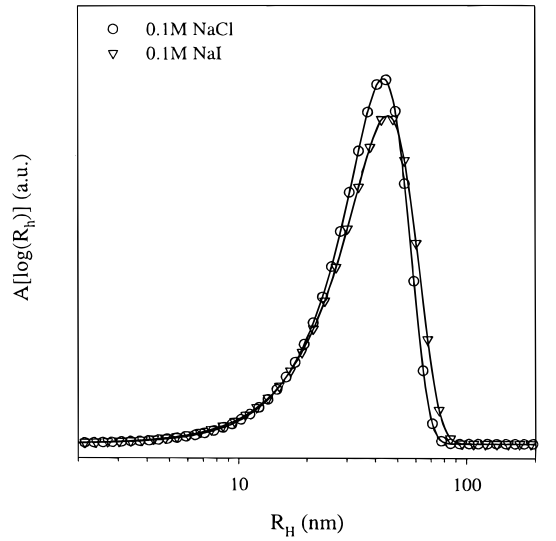

Figure 5. Size distribution of κ-carrageenan solutions in 0.1 M NaCl and 0.1 M NaI at 20 °C.

between the size distributions in the coil and helix conformation.

The characterization of the large κ-carrageenan sample studied here shows that the molar mass is the same in the coil and the helix state which suggests simple helix formation in agreement with the conclusion of Bongaerts et al.[21] Both static and dynamic light scattering show that the size of κ-carrageenan is not very different in the coil and helix conformation. On the other hand, Slootmaekers et al.[19,20] observed an increase in size of about 25% in the helical form. At the present moment we have no explanation for this observation which is clearly outside the experimental uncertainty of the results presented here. The coil−helix transition has two opposing effects on the overall size of the chains: the chain length is reduced in the helical form, which reduces the size while the larger persistence length in the helical form increases the size. It appears that the total effect on the overall size is small.

The static and dynamic virial coefficients are smaller in NaI than in NaCl as was reported earlier by Slootmaekers et al.[19,20] However, as mentioned in the Introduction, it has been suggested that κ-carrageenan reversibly associates in the presence of NaI so that the molar mass increases with increasing concentration.[17] In the calculation of A_2 and k_d we assumed that the molar mass is independent of C. Even though the effect was only clearly observed with ionic strength 0.2 M and higher, a weak effect of association might explain the lower apparent virial coefficients.

Structure of κ-Carrageenan Aggregates. In the presence of 0.01 M KCl, κ-carrageenan has a coil−helix transition which starts at T_c = 24 °C but is only complete below the freezing point of water. This is shown by the variation with temperature of the specific optical rotation ([α]); see Figure 1. The temperature dependence of [α] is independent of the κ-carrageenan concentration at least over the range studied here. As mentioned in the Experimental Section, the solutions contain in addition to 0.01 M KCl also 0.1 M NaCl in order to reduce electrostatic interactions. The presence of 0.1 NaCl does not significantly modify the temperature dependence of [α]; see Figure 1. In KCl the coil−helix transition induces aggregation of κ-carrageenan and eventually gel formation. In the following we investigate the evolution of the structure of the aggregates at different concentrations and temperatures.

Time Dependence. Figure 6 shows the evolution of the excess scattering intensity and the temperature of a κ-carrageenan solution taken from the oven at 50 °C and introduced in the light scattering apparatus set at 15 °C. As soon as the temperature decreases below T_c, I_r increases. Initially the increase is rapid, but the log−log representation shows that the increase continues for a very long time without showing any sign of reaching a steady state. The continuous slow evolution of I_r is in sharp contrast with that of the optical rotation which reaches a steady value within a minute at a given temperature. This implies that aggregation does not modify the local conformation of the κ-carrageenan chains.

To obtain I_r over a range of q we have measured the intensity for short periods at successive angles of observation. For two q values we followed the intensity

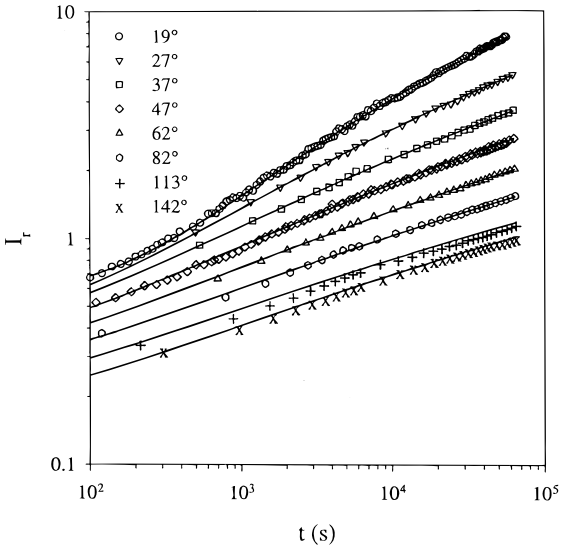

Figure 7. Evolution of the relative excess scattering intensity ($C = 0.1$ g/L, $T = 15$ °C, 0.01 M KCl, 0.1 M NaCl) at different angles indicated in the figure ($q = 5.20 \times 10^{-3}$ to 2.98×10^{-2} nm^{-1}). The solid lines are guides to the eye.

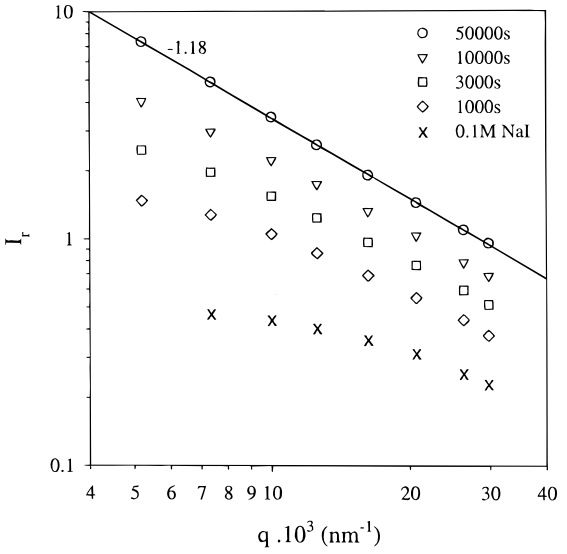

Figure 8. q dependence of the relative excess scattering intensity ($C = 0.1$ g/L, $T = 15$ °C, 0.01 M KCl, 0.1 M NaCl) at different times. The solid line represents a linear least-squares fit. The crosses show the q dependence of κ-carrageenan in the nonaggregated helix conformation (0.1 M NaI).

continuously in repeat measurements. Clearly, the intensity continues to increase over the whole q range investigated even after long times; see Figure 7. We have chosen the time where I_r starts to increase, t_0, as the start of the aggregation process and have subtracted t_0 from the total time in order to represent the evolution of I_r as a function of the aggregation time in Figure 7 and subsequent figures. Unfortunately, the equilibration of the temperature is not very rapid with the setup used here, which means that the evolution during the first 2000 s is not well defined.

The q dependence of I_r at different aggregation times was obtained by interpolation and is shown in Figure 8. For comparison, we also show the q dependence of the nonaggregated helices in 0.1 M NaI. Already after relatively short aggregation times the q dependence of I_r is too strong to allow an analysis in terms of the Zimm approximation. At long times I_r is no longer sensitive

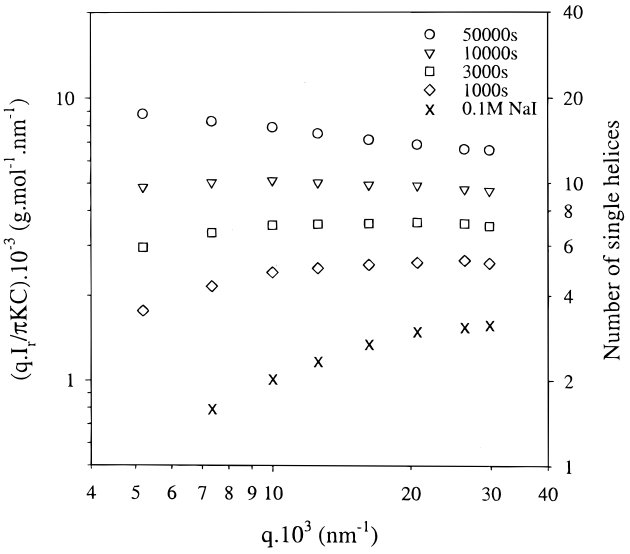

Figure 9. q dependence of $qI_r/\pi KC$ at different times intensity ($C = 0.1$ g/L, $T = 15$ °C, 0.01 M KCl, 0.1 M NaCl). For comparison we show on the left axis the values of $qI_r/\pi KC$ corresponding to long aggregates with the diameter expressed in units of thickness of a single helix.

to the overall size of the aggregates in the q range probed in this experiment, and the q dependence is a measure only of the internal structure of the aggregates. The q dependence of I_r at long times can be approximated by a power law dependence with an exponent close to unity. This suggests a rigid-rod-like local structure for the aggregates. For noninteracting rigid rods with length L and diameter d the weight-average molar mass per unit length, M_L, is given by[23]

$$M_L = \frac{qI_r}{\pi KC} \quad (L \gg q^{-1} \gg d) \tag{8}$$

For semiflexible polymers eq 7 is only valid for q^{-1} much smaller than the persistence length (l_p). In Figure 9 we have plotted $qI_r/\pi KC$ as a function of q. At large q values $qI_r/\pi KC$ becomes constant and can be interpreted as the molar mass per unit length. We will show below that in the concentration used here interactions between the aggregates can be neglected over the accessible q range. M_L increases continuously with aggregation time which explains why I_r increases even if $qR_{gz} \gg 1$.

On the basis of X-ray scattering,[12−14] we have calculated that $M_L \approx 500$ g/(mol nm) for a single helix. If we assume that all κ-carrageenan is present in the form of stacked single helices, we find that the parallel aggregation number increases from about 5 to about 12 over the period investigated. Of course, it is possible that part of the κ-carrageenan is not in the form of stacked helices, especially at short times. This means that the true parallel aggregation number may be somewhat larger. The cross section of the aggregates remains too small to have a significant influence on the q dependence in the accessible range.

For the smaller aggregates, $qI_r/\pi KC$ increases with q at low q values due to the finite size of the particles. For the large aggregates formed at longer times, it decreases with q at low q, implying a denser large scale structure. One possible interpretation of the data would be to treat the aggregates as semiflexible polymers. Unfortunately, no general analytical expression exists for the structure factor of semiflexible polymers. Ped-

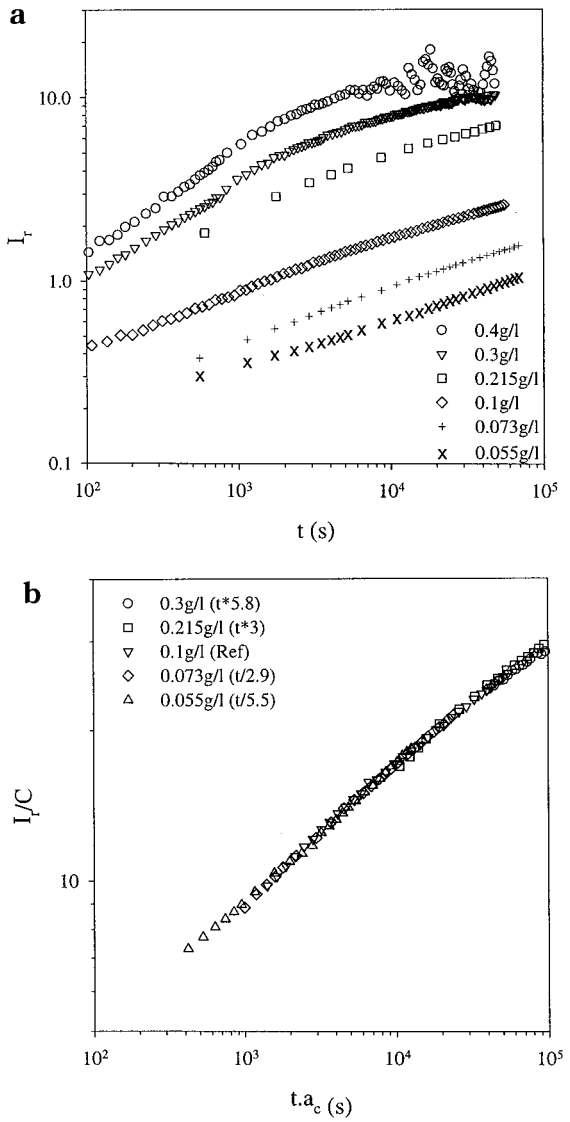

Figure 10. (a) Time evolution of the relative excess scattering intensity at different concentrations indicated in the figure ($q = 2.06 \times 10^{-2}$ nm^{-1}, $T = 15$ °C, 0.01 M KCl, 0.1 M NaCl). (b) Master curve of data shown in (a) obtained by normalization with the concentration and horizontal shifts with $C_{ref} = 0.1$ g/L. Shift factors and concentrations are indicated in the figure.

ersen et al.[33] have given a cumbersome analytical expression that fits their simulation results. However, it is doubtful that an analysis in terms of this expression gives more than very rough estimates of the radius of gyration and the persistence length in view of the unknown polydispersity in the length and the cross section of the aggregates. By simply considering the weak q dependence in Figure 9 at long times, we estimate that the persistence length must be at least a few hundred nanometers.

Another possible origin for the weak deviation from the rigid-rod q dependence at low q values is junctions between the parallel stacked bundles which would lead to a denser large-scale structure. The existence of junctions seems to be implied by the fact that the aggregation leads to the formation of a nonflowing gel. The strength of the gel increases with increasing concentration, and at high concentrations one even observes syneresis. However, the nature of the junctions is as yet unknown. Whatever their nature, they must be relatively rare to have such a weak influence on the

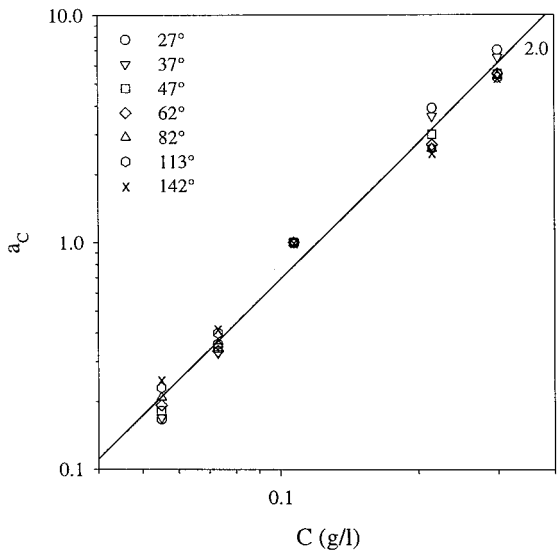

Figure 11. Concentration dependence of the horizontal shift factors a_C used to obtain master curves at different angles of observation. The solid line has slope two.

q dependence. We note in passing that an early model of the κ-carrageenan gel suggested by Rees[1] is in contradiction with the present results. In this model it was assumed that one κ-carrageenan chain forms a double helix with more than one other chain and that no parallel aggregation occurs.

Concentration Dependence. In Figure 10a we show the evolution of I_r at different concentrations. Clearly, the aggregation rate increases with increasing concentration. We limit the investigation here to rather low concentrations because at higher concentrations a gel is formed already after relatively short times which leads to very slow intensity fluctuations; see for example the solution at $C = 0.4$ g/L in Figure 10a. We will discus the origin of these slow fluctuations elsewhere.

The q dependence of I_r, i.e., $S(q)$, can be influenced both by interactions and by a change of the aggregate structure. To investigate whether the internal structure of large aggregates is concentration-dependent, we have to correct for the concentration-dependent aggregation rate. If the difference in the evolution of I_r is only due to the variation of the aggregation kinetics, then it should be possible to superimpose the evolution of I_r/C obtained at different concentrations by simple time shifts. The superposition is shown in Figure 10b and works well if we use only times longer than the time needed for temperature equilibrium. Similar curves were obtained over a range of q values. The shift factors (a_C) used in the superposition are plotted as a function of the concentration in Figure 11. The shift factors are the same over the whole q range investigated which suggests that the evolution of the structure factor is independent of the concentration. This means that the effect of interactions is small in the concentration range investigated.

The concentration dependence of the shift factors represents the concentration dependence of the aggregation rate if it is true that only the rate of aggregation is influenced by the concentration but not the structure factor of the aggregates. The solid line in Figure 11 represents $a_C \propto C^2$, which is in agreement with the concentration dependence of the relaxation rate that was obtained from viscoelastic measurements at higher concentrations.[18] Note that this dependence of

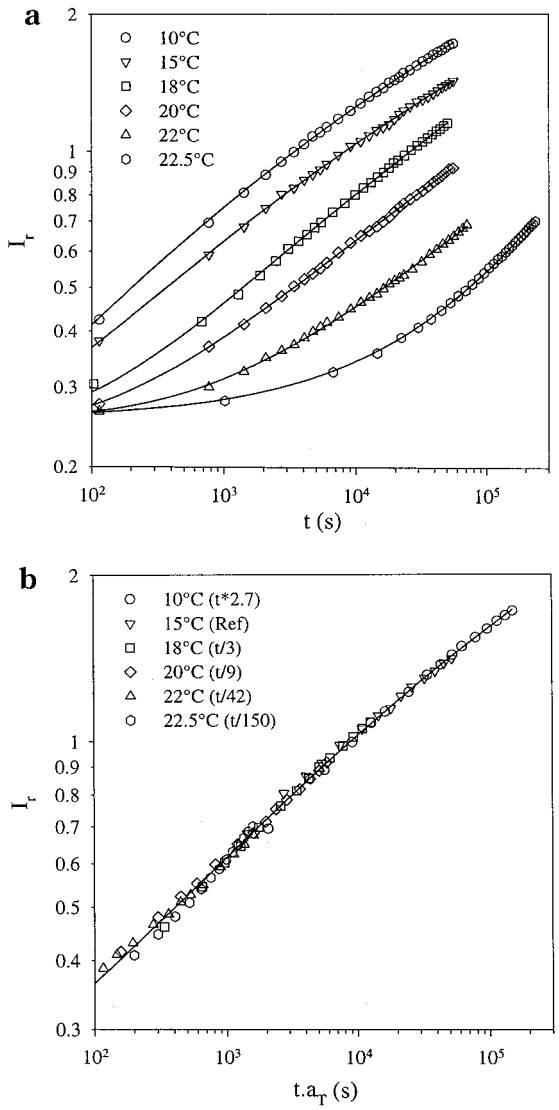

Figure 12. (a) Time evolution of the relative excess scattering intensity ($C = 0.1$ g/L, $q = 2.06 \times 10^{-2}$ nm^{-1}, 0.01 M KCl, 0.1 M NaCl) at different temperatures indicated in figure. The solid lines are guides to the eye. (b) Master curve of the data shown in (a) obtained by horizontal shifts with $T_{ref} = 15$ °C. Shift factors and temperatures are indicated in the figure.

the aggregation rate does not necessarily imply that the rate-limiting step is a simple binary reaction between previously formed helices. The observed simple overall concentration dependence could hide a complicated mechanism.

Temperature Dependence. In Figure 12a we show the evolution of I_r at $C = 0.1$ g/L at different temperatures. All data can be superimposed by simple horizontal shifts; see Figure 12b. Master curves could be obtained in this way at all q values investigated. The shift factors (a_T) used to obtain the master curves are plotted as a function of temperature in Figure 13. The shift factors are independent of q, which confirms the conclusion of our earlier study that the temperature only influences the aggregation rate but not the structure of the aggregates.[18] In addition, as mentioned above, polarimetry shows that the fraction of segments in the helical conformation (F) does not change during the aggregation. These observations imply that the same aggregates are formed regardless the value of F although more slowly if F is smaller. We have seen that the aggregation process can be viewed as a simple parallel stacking of

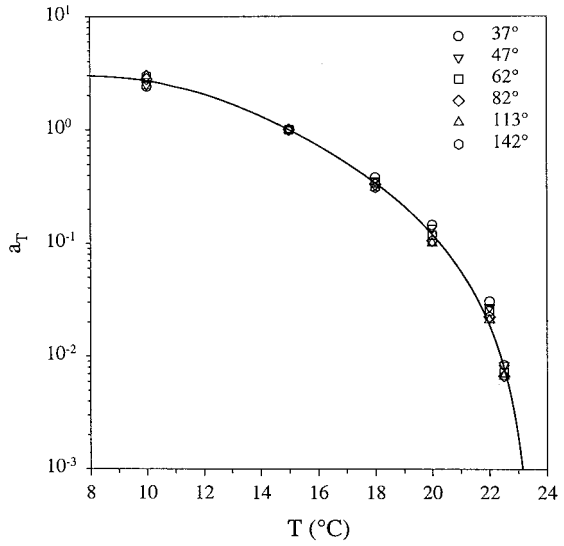

Figure 13. Temperature dependence of the horizontal shift factors a_T used to obtain the master curves at different values angles of observation. The solid lines are guides to the eye.

κ-carrageenan chains, but apparently they need not be fully in the helical conformation.

In our analysis we have assumed that the fraction of segments in the helical conformation at a given temperature is equally distributed over all κ-carrageenan chains. Instead, it might be argued that a fraction of the chains is still fully in the coil state and therefore does not aggregate. The extreme position would be that the solutions contain two discrete populations of chains that either have the maximum helical conformation or are fully in the coil state. With optical rotation one cannot distinguish between these possibilities, because it probes the conformation on a local length scale. Therefore, we reanalyzed the data assuming the double population; i.e., we subtracted the contribution of κ-carrageenan in the coil state and divided I_r by F. However, with this procedure the curves at different temperatures could not be superimposed by horizontal shifts and even crossed at long times; i.e., the scattering of the aggregates at temperatures closer to T_c becomes larger. We believe that the extreme case of a double population of κ-carrageenan in the coil state or helix state is unlikely. But, of course, we do not exclude the possibility that a small fraction of chains is still fully in the coil state.

The temperature dependence of the aggregation rate is much stronger than that of F or even F^2. We have found approximately $a_T \propto F^4$. If a discrete double population is assumed, F is proportional to the concentration of κ-carrageenan in the helical conformation that can participate in the aggregation, and one would expect $a_T \propto F^2$.

Conclusions

The molar mass and size of high molar mass non-aggregated κ-carrageenan are not very different in the coil and the helix state.

In the presence of KCl, κ-carrageenan aggregates by parallel stacking of the chains. The local structure is rigid up until length scales of a few hundred nanometers. The parallel stacking increases continuously, and in the concentration (0.05−0.3 g/L) and temperature ($T_c - T < 15$) range tested equilibrium was not reached in a period of 16 h. However, the long time aggregation is

very slow, and the largest number of parallel stacked κ-carrageenan chains reached in the experiments corresponds to about 13 simple helices.

The structure of aggregates with a given molar mass is independent of the temperature and the concentration at least for $C < 0.3$ g/L. The aggregation rate increases approximately with the square of the concentration. The temperature dependence of the aggregation rate is much stronger than that of the optical rotation.

Acknowledgment. We thank SKW Biosystems for financial support and Dr. M. Djabourov at ESPCI for use of a polarimeter.

References and Notes

(1) Rees, D. A. *Adv. Carbohydr. Chem.* **1969**, *24*, 267.
(2) Amat, M. A. *Oceanis* **1989**, *15*, 661.
(3) Trius, A.; Sebranek, J. G. *Food Sci. Nutr.* **1996**, *36*, 69.
(4) Rees, D. A.; Steele, I. W.; Williamson, F. B. *J. Polym. Sci.* **1969**, *28*, 261.
(5) Paoletti, S.; Delben, F.; Cesaro, A.; Grasdalen, H. *Macromolecules* **1985**, *18*, 1834.
(6) Morris, E. R.; Rees, D. A.; Robinson, G. *J. Mol. Biol.* **1980**, *138*, 349.
(7) Rochas, C.; Landry, S. *Carbohydr. Polym.* **1987**, *7*, 435.
(8) Norton, I. T.; Goodall, D. M. *J. Chem. Soc.* **1983**, *79*, 2475.
(9) Ueda, K.; Itoh, M.; Matsuzaki, Y.; Ochiai, H.; Imamura, A. *Macromolecules* **1998**, *31*, 675.
(10) Nerdal, W.; Haugen, F.; Knutsen, S.; Grasdalen, H. *J. Biomol. Struct. Dyn.* **1993**, *10*, 785.
(11) Vanneste, K.; Mandel, M.; Paoletti, S.; Reynaers, H. *Macromolecules* **1994**, *27*, 7496.
(12) Bayley, S. T. *Biochim. Biophys. Acta* **1955**, *17*, 194.
(13) Anderson, N. S.; Campbell, J. W.; Harding, S. E.; Rees, D. A.; et al. *J. Mol. Biol.* **1969**, *45*, 85.
(14) Millane, R. P.; Chandrasekaran, R.; Arnott, S.; Dea, I. C. M. *Carbohydr. Res.* **1988**, *182*, 1.
(15) Borgström, J.; Piculell, L.; Viebke, C.; Talmon, Y. *Int. J. Biol. Macromol.* **1996**, *18*, 223.
(16) Morris, V. J.; Gunning, A. P.; Kirby, A. R.; Round, A.; et al. *Int. J. Biol. Macromol.* **1997**, *21*, 61.
(17) Bongaerst, K.; Reynaers, H.; Zanetti, F.; Paoletti, S. *Macromolecules* **1999**, *32*, 683.
(18) Meunier, V.; Nicolai, T.; Durand, D.; Parker, A. *Macromolecules* **1999**, *32*, 2610.
(19) Slootmaekers, D.; De Jonghe, C.; Reynaers, H.; Varkevisser, F. A.; Bloys van Treslong, C. J. *Int. J. Biol. Macromol.* **1988**, *10*, 160.
(20) Slootmaekers, D.; Mandel, M.; Reynaers, H. *Int. J. Biol. Macromol.* **1991**, *13*, 17.
(21) Bongaerst, K.; Reynaers, H.; Zanetti, F.; Paoletti, S. *Macromolecules* **1999**, *32*, 675.
(22) Hjerde, T.; Smidsrod, O.; Christensen, B. E. *Biopolymers* **1999**, *49*, 71.
(23) *Light Scattering from Polymer Solutions*; Huglin, Ed.; Academic Press: London, 1972. Higgins, J. S.; Benoit, K. C. *Polymers and Neutron Scattering*; Clarendon Press: Oxford, 1994. *Light Scattering. Principles and Developments*; Brown, W., Ed.; Clarendon Press: Oxford, 1996.
(24) Finnigan, J. A.; Jacobs, D. J. *Chem. Phys. Lett.* **1970**, *6*, 141. Moreels, E.; De Ceunick, W. *J. Chem. Phys.* **1987**, *86*, 618.
(25) Berne, B.; Pecora, R. *Dynamic Light Scattering*; Wiley: New York, 1976.
(26) Stepanek, P. In *Dynamic Light Scattering*; Brown, W.; Ed.; Oxford University Press: New York, 1993; Chapter 4.
(27) Nicolai, T.; Gimel J. C.; Johnsen, R. *J. Phys. II* **1996**, *6*, 697.
(28) Busnel, J. P.; Degoulet, C.; Nicolai, T.; Woodley, W.; Patin, P. *J. Phys. III* **1995**, *5*, 1501.
(29) Ekström, L.-G. *Carbohydr. Res.* **1985**, *135*, 283.
(30) Hjerde, T.; Smidsrod, O.; Christensen, B. E. *Carbohydr. Res.* **1996**, *288*, 175.
(31) Rochas, C.; Heyraud, A. *Polym. Bull.* **1981**, *5*, 81.
(32) Rochas, C.; Rinaudo, M. *Biopolymers* **1984**, *23*, 735.
(33) Pedersen, J. S.; Laso, M.; Schurtenberger, P. *Phys. Rev. E* **1996**, *54*, 5917.

MA991433T